Chaos, Solitons & Fractals 45 (2012) 294–305

Contents lists available at SciVerse ScienceDirect

Chaos, Solitons & Fractals

Nonlinear Science, and Nonequilibrium and Complex Phenomena

journal homepage: www.elsevier.com/locate/chaos

Ternary choices in repeated games and border collision bifurcations

Arianna Dal Forno [a,*], Laura Gardini [b], Ugo Merlone [c]

[a] Department of Statistics and Applied Mathematics, University of Torino, Italy
[b] Department of Economics, Society and Politics, University of Urbino, Italy
[c] Department of Psychology, University of Torino, Italy

ARTICLE INFO

Article history:
Received 29 January 2011
Accepted 5 December 2011

ABSTRACT

Several recent contributions formalize and analyze *binary choices games with externalities* as those described by Schelling. Nevertheless, in the real world choices are not always binary, and players have often to decide among more than two alternatives. These kinds of interactions are examined in game theory where, starting from the well known rock-paper-scissor game, several other kinds of strategic interactions involving more than two choices are examined. In this paper we investigate how the dynamics evolve introducing one more option in binary choice games with externalities. The dynamics we obtain are always in a stable regime, that is, the structurally stable dynamics are only attracting cycles, but of any possible positive integer as period. We show that, depending on the structure of the game, the dynamics can be quite different from those existing when considering binary choices. The bifurcation structure, due to border collisions, is explained, showing the existence of so-called big-bang bifurcation points.

1. Introduction

The problem of repeated choices has been studied from different perspectives, especially in economics. For example in [8] the first chapter is devoted to the theory of individual decision making. According to these Authors "The starting point for any individual decision problem is a *set of possible (mutually exclusive) alternatives* from which the individual must choose". In many texts (see e.g. [13]), for the sake of simplicity, the analysis is limited to choices between two alternatives such as consumption goods. In an important contribution appeared in the Journal of Conflict Resolution, Schelling [10] analyzes situations in which the consequences of the choices of an actor are affected by other actors' actions, that is, the population of agents that form the social system as a whole. In particular, he considers agents who are asked to choose between two alternatives and each player's payoff depends on the number of agents who choose either one action or the other. These kinds of interaction are called *binary choices games with externalities*.

Recently, after providing a mathematical formalization, the analysis provided in [2] extends Schelling's contribution introducing a dynamic adjustment process. The dynamics was analyzed thoroughly in [3] where the analytic expressions of the border collision bifurcation curves are given. Furthermore, [4] extends such analysis considering the case in which the payoff functions have two intersections as in some examples provided in Schelling [10]. In this case the one-dimensional map consists of three linear partitions separated by two discontinuity points.

Nevertheless, in the real world the choice set does not always consist of two alternatives. This is well known in economics, for example [9] when surveying quantal choice analysis provides a classical illustration. The example is the following: "... suppose subjects are offered a choice of a bicycle or a pony.... Suppose the choice is now expanded to include a second bicycle which differs from the first only in color and trim." Examples considering more than two choices are not limited to quantal choice analysis; game theory also examines situations in which players have at

* Corresponding author. Address: Dipartimento di Statistica e Matematica Applicata, Corso U. Sovietica 218/bis, I-10134 Torino, Italy. Tel.: +39 011 3177119; fax: +39 011 6705783.
E-mail addresses: dalforno@econ.unito.it (A. Dal Forno), laura.gardini@uniurb.it (L. Gardini), ugo.merlone@unito.it (U. Merlone).

0960-0779/$ - see front matter © 2011 Elsevier Ltd. All rights reserved.
doi:10.1016/j.chaos.2011.12.003

least three available alternatives. In [5], several examples are provided, from pricing games with price matching to sport examples. Furthermore, even for simple games such as the well known rock-paper-scissor, externalities effects arise when they are played as stage games in random matching supergames [7]. Finally, it is also possible to obtain an example similar to those provided in [10] when considering the dilemma of commuting by car or public transportation examined in [12], and introducing a third choice: commuting by bicycle.

In this paper we investigate how introducing one more option in binary choices games with externalities affects the complexity of the dynamics. We will show that, depending on the structure of the game in terms of the payoff, the dynamics can be more complex than the one when considering binary choices.

The choice of linear payoff functions will lead to two-dimensional maps defined by linear pieces. Thus the dynamics shown via several examples is the one typical of piecewise linear maps with one or two discontinuity sets. In these maps the bifurcations are different from those occurring in smooth systems, and are due to the collision of some cycle with the border in which the definitions change. The effect of such a border collision bifurcation is not an easy task to investigate, especially in two-dimensional piecewise linear maps. It is indeed an open research field, in which only a few results have been published, and mainly for continuous piecewise smooth maps. For discontinuous maps, as it is in our model, the existing results are almost negligible. However, the examples considered in this work allows us to investigate the bifurcations via a one-dimensional discontinuous map. In such a case we are able to understand and classify the bifurcations occurring in the map (making use of recent results in [6,1,11]).

Our results show how considering binary choices to simplify the problem formulation may lead to miss the complex dynamics of the system under analysis, although the structurally stable attracting set always consists in some k-cycle, $k \geqslant 1$, as *divergent dynamics or chaotic behaviors cannot occur*.

The structure of the paper is the following. The model is presented in Section 2. The analysis proceeds from the case of only stable equilibria (Section 3), through the examination of the coexistence of a stable equilibrium and cycles (Section 4). The cases shown here can be considered as reflecting the result of two choices plus one. Differently, in Section 5 we shall illustrate a case in which the three different choices are cyclically changing, which occurs when there are no stable equilibria. Section 6 is devoted to the conclusions and open problems.

2. The model

We consider a repeated game where a continuum of players chooses actions from a set $A = \{L,M,R\}$. Each player updates its choice at each time $t = 0,1,2,\ldots$. The set of players is normalized to the interval $[0,1]$. We introduce the following notation:

- $x_t^L \in [0,1]$ denotes the fraction of players choosing action L at time t,
- $x_t^M \in [0,1]$ denotes the fraction of players choosing action M at time t,
- $x_t^R \in [0,1]$ denotes the fraction of players choosing action R at time t.

Since we are considering ternary choices, when at any time t a fraction x_t^L of the population chooses action L and a fraction x_t^R chooses action R, then a fraction $x_t^M = 1 - x_t^L - x_t^R$ chooses action M. We rule out the option of not choosing any action. As it holds $x_t^L + x_t^M + x_t^R = 1$ it is possible to represent the state of the system on Δ^2, the standard 2-simplex with vertices $P_L^*(1,0,0), P_M^*(0,1,0), P_R^*(0,0,1)$, as in Fig. 1(a).

Assuming $x_t^M = 1 - x_t^L - x_t^R$ it is possible to consider only two independent coordinates (x_t^L, x_t^R) and in the following we will omit x^M (given as complement value).

Thus our phase space (the set of feasible vectors $\mathbf{x}_t = (x_t^L, x_t^R)$) is a triangle D^2 in the plane which has to be considered as the projection (bijective) of the standard 2-simplex Δ^2:

$$D^2 = \left\{\mathbf{x}_t = (x_t^L, x_t^R) \in \mathbb{R}^2 : 0 \leqslant x_t^L + x_t^R \leqslant 1\right\}.$$

Therefore the vertices of Δ^2 become the vertices of D^2:

$$P_L^* = (1,0), \quad P_M^* = (0,0), \quad P_R^* = (0,1), \tag{1}$$

respectively, as depicted in Fig. 1(b).

Obviously:

- if $\mathbf{x}_t = (x_t^L, x_t^R) = (0,0)$ then the whole population chooses action M,
- if $\mathbf{x}_t = (x_t^L, x_t^R) = (0,1)$ then the whole population chooses action R,
- if $\mathbf{x}_t = (x_t^L, x_t^R) = (1,0)$ then the whole population chooses action L.

They can be named *unanimity* vertices since in each of them the whole population is choosing the same action.

The payoff functions are common knowledge and are assumed to be linear functions depending on the vector $\mathbf{x} = (x^L, x^R)$; they are:

- $L : D^2 \to \mathbb{R}$ is the payoff associated to action L:

$$L(\mathbf{x}) = a_L x^L + b_L x^R + c_L, \tag{2}$$

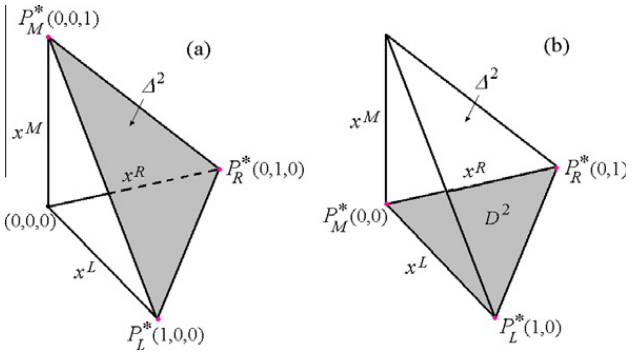

Fig. 1. In (a) standard 2-simplex Δ^2 (shaded area) and in (b) its projection D^2 on the horizontal plane (shaded area).

- $M : D^2 \to \mathbb{R}$ is the payoff associated to action M:

$$M(\mathbf{x}) = a_M x^L + b_M x^R + c_M, \tag{3}$$

- $R : D^2 \to \mathbb{R}$ is the payoff associated to action R:

$$R(\mathbf{x}) = a_R x^L + b_R x^R + c_R. \tag{4}$$

We assume that each pair of payoff functions are not identically the same. Then defining:

$$\begin{aligned} T_1(\mathbf{x}) &= L(\mathbf{x}) - M(\mathbf{x}) = (a_L - a_M)x^L + (b_L - b_M)x^R + (c_L - c_M),\\ T_2(\mathbf{x}) &= L(\mathbf{x}) - R(\mathbf{x}) = (a_L - a_R)x^L + (b_L - b_R)x^R + (c_L - c_R),\\ T_3(\mathbf{x}) &= R(\mathbf{x}) - M(\mathbf{x}) = (a_R - a_M)x^L + (b_R - b_M)x^R + (c_R - c_M). \end{aligned} \tag{5}$$

We are interested in the following regions:

$$\begin{aligned} R_L &= \left\{\mathbf{x} \in D^2 : \quad T_1(\mathbf{x}) > 0 \quad \text{and} \quad T_2(\mathbf{x}) > 0\right\},\\ R_M &= \left\{\mathbf{x} \in D^2 : \quad T_1(\mathbf{x}) < 0 \quad \text{and} \quad T_3(\mathbf{x}) < 0\right\},\\ R_R &= \left\{\mathbf{x} \in D^2 : \quad T_2(\mathbf{x}) < 0 \quad \text{and} \quad T_3(\mathbf{x}) > 0\right\}. \end{aligned} \tag{6}$$

We assume that not all these sets are empty, in which case the regions are convex, as intersection of convex sets. In the region R_L we have that action L dominates both M and R; in R_M action M dominates the other payoffs L and R; and in R_R it is R that dominates L and M. As usual, the set of feasible vectors $\mathbf{x}_t = (x_t^L, x_t^R)$ are such that $x_t^L + x_t^R \leqslant 1$ for all t.

The agents are homogeneous and maximize their next period utility. At time $t+1$ vector $\mathbf{x}_t$ becomes common knowledge, and each agent can observe payoffs $L(\mathbf{x}_t)$, $M(\mathbf{x}_t)$ and $R(\mathbf{x}_t)$. We assume that if at time t a fraction x_t^L chooses action L and a fraction x_t^R chooses action R and the payoffs are such that $R(\mathbf{x}_t) > L(\mathbf{x}_t)$ and $R(\mathbf{x}_t) > M(\mathbf{x}_t)$, then a fraction of the x_t^L agents who chose action L and a fraction of the $1 - x_t^L - x_t^R$ agents who chose action M will both switch to action R at next time period $t+1$. This is the same for all actions which give the larger payoff. In other words, at any time t all the agents decide their future action for time $t+1$ comparing payoffs $L(\mathbf{x}_t)$, $M(\mathbf{x}_t)$ and $R(\mathbf{x}_t)$ according to the following rule:

$$\mathbf{x}_{t+1} = \mathbf{F}(\mathbf{x}_t) \tag{7}$$

with $\mathbf{x}_t = (x_t^L, x_t^R) \in \mathbb{R}^2$, $\mathbf{F}$: $D^2 \to D^2$ and the map:

$$(x_{t+1}^L, x_{t+1}^R) = (F_L(\mathbf{x}_t),\ F_R(\mathbf{x}_t)) \tag{8}$$

is defined as follows:

- if $\mathbf{x}_t \in R_L$ then:

$$\begin{cases} F_L(\mathbf{x}_t) = x_t^L + \delta_L g(\lambda(L(\mathbf{x}_t) - M(\mathbf{x}_t)))\left(1 - x_t^L - x_t^R\right) + \delta_L g(\lambda(L(\mathbf{x}_t) - R(\mathbf{x}_t)))x_t^R,\\ F_R(\mathbf{x}_t) = x_t^R - \delta_L g(\lambda(L(\mathbf{x}_t) - R(\mathbf{x}_t)))x_t^R, \end{cases}$$

- if $\mathbf{x}_t \in R_M$ then:

$$\begin{cases} F_L(\mathbf{x}_t) = x_t^L - \delta_M g(\lambda(M(\mathbf{x}_t) - L(\mathbf{x}_t)))x_t^L,\\ F_R(\mathbf{x}_t) = x_t^R - \delta_M g(\lambda(M(\mathbf{x}_t) - R(\mathbf{x}_t)))x_t^R, \end{cases}$$

- if $\mathbf{x}_t \in R_R$ then:

$$\begin{cases} F_L(\mathbf{x}_t) = x_t^L - \delta_R g(\lambda(R(\mathbf{x}_t) - L(\mathbf{x}_t)))x_t^L,\\ F_R(\mathbf{x}_t) = x_t^R + \delta_R g(\lambda(R(\mathbf{x}_t) - L(\mathbf{x}_t)))x_t^L + \delta_R g(\lambda(R(\mathbf{x}_t) - M(\mathbf{x}_t)))\left(1 - x_t^L - x_t^R\right). \end{cases}$$

The function $g : \mathbb{R}_+ \to [0,1]$ is *continuous and increasing*, with $g(0) = 0$ and $\lim_{z\to+\infty} g(z) = 1$; it models the impulsivity of agents (see [3]), as the parameter $\lambda \in \mathbb{R}_+$ represents the agents' speed of reaction as a consequence of the comparison between the payoffs.

The parameters δ_L, δ_M, and δ_R, assumed belonging to the range $[0,1]$, represent how many agents may switch to action L, M, and R respectively. When two or more of these parameters are equal, there are no differences in the propensity to switch to any of the actions involved.

An interesting limiting case is obtained as λ goes to infinity, as considered in [3]. This is equivalent to consider $g(\cdot) = 1$. Therefore, the switching rate to a different action just depends on the sign of the difference between the payoffs, no matter to what extent (impulsive agents). In this case the dynamical system becomes $\mathbf{x}_{t+1} = \overline{\mathbf{F}}(\mathbf{x}_t)$ as follows:

$$\overline{\mathbf{F}}: \quad \mathbf{x}_{t+1} = \begin{cases} \begin{cases} x_{t+1}^L = (1-\delta_L)x_t^L + \delta_L\\ x_{t+1}^R = (1-\delta_L)x_t^R \end{cases} & \text{if} \quad \mathbf{x}_t \in R_L,\\ \begin{cases} x_{t+1}^L = (1-\delta_M)x_t^L\\ x_{t+1}^R = (1-\delta_M)x_t^R \end{cases} & \text{if} \quad \mathbf{x}_t \in R_M,\\ \begin{cases} x_{t+1}^L = (1-\delta_R)x_t^L\\ x_{t+1}^R = (1-\delta_R)x_t^R + \delta_R \end{cases} & \text{if} \quad \mathbf{x}_t \in R_R. \end{cases} \tag{9}$$

We can see that in the map in (9), each of the expressions defining x_{t+1}^L and x_{t+1}^R is a linear function only of the same state variable, and not of the other one. However, depending on the payoff values, the state variable may change the region to which it belongs to, and this leads to a change in the dynamics. That is, the function which is applied to the state variables changes as a consequence of the change of the region.

The peculiarity of this two-dimensional map $\overline{\mathbf{F}}$ is that the conditions on the parameters determining the slopes of the linear functions, and thus the eigenvalues of the map in the linear pieces, lead to all contractions. A point $\mathbf{x} \in R_\sigma$ has the Jacobian matrix:

$$J(x^L, x^R) = \begin{pmatrix} 1-\delta_\sigma & 0\\ 0 & 1-\delta_\sigma \end{pmatrix},$$

whose eigenvalues are real and both equal to $(1-\delta_\sigma)$, so that they belong to the range $(0,1]$, except for $\delta_\sigma = 0$, in which case the eigenvalues are both equal to 1.

Under such conditions we can only have stable cycles,[1] as all the eigenvalues of the components are positive and less then one, or at most equal to 1, any possible $k-$periodic cycle ($k \geqslant 1$) has eigenvalues which are necessarily also positive and smaller than or equal to one.[2] Thus no chaotic behavior can occur, neither divergence (as the map is defined from D^2 onto D^2). We have so proved the following:

[1] Except for particular structurally unstable parameter values at which quasiperiodic trajectories exist.

[2] We recall that the eigenvalues of a cycle are given by the eigenvalues of the product of the Jacobian matrices in the periodic points.

Proposition 1. *The map* $\overline{\mathbf{F}}$ *in (9) can only have regular dynamics: either* $k-$*cycles for any* $k \geqslant 1$ *or quasiperiodic trajectories.*

In the next sections we shall see several examples. There, the particular structure of the map often leads to one-dimensional maps by which it is possible to analyze the dynamic behaviors and bifurcations which may occur. Also, it may happen that, depending on the structure of the regions, we can have one of the two state variables independent from the other. An example is given in Section 5.

3. Analysis of stable fixed points

When in any of the three vertices, $P^*_\sigma, \sigma \in \{L, M, R\}$, the correspondent payoff dominates the others, then such a vertex may be a stable fixed point. P^*_σ is a real fixed point if it belongs to the proper region R_σ, otherwise is called virtual. In fact, if $P^*_\sigma \in R_\sigma$ then, given the definition of the map in (9), it attracts all the points in its region. In other words, a unanimity vertex is locally stable iff it belongs to the related dominance region, as proved in the following proposition.

Proposition 2. *A vertex* P^*_σ *of* D^2 *is a stable fixed point if* $P^*_\sigma \in R_\sigma$*, where* $\sigma \in \{L, M, R\}$*, and explicitly:*

$$
\begin{aligned}
&P^*_L \in R_L \quad \text{if } (a_L + c_L) > \max(a_M + c_M, a_R + c_R),\\
&P^*_M \in R_M \quad \text{if } c_M > \max(c_L, c_R),\\
&P^*_R \in R_R \quad \text{if } (b_R + c_R) > \max(b_L + c_L, b_M + c_M).
\end{aligned}
$$

Proof. Given the definition of the map in (9) it is immediate to observe that a unanimity vertex P^*_σ which belongs to the related region is a fixed point, as $\mathbf{x}_t = P^*_\sigma$ implies $\mathbf{x}_{t+1} = P^*_\sigma$, and it attracts all the points in its region. In fact, since the eigenvalues are both equal to $(1 - \delta_\sigma)$ and in the range $[0,1]$, a point $\mathbf{x}_t \in R_\sigma$ implies $\mathbf{x}_{t+1} \in R_\sigma$. As a consequence, for $0 < \delta_\sigma \leqslant 1$, P^*_σ is an attracting fixed point with monotonic convergence, and from the structure of the map the trajectories belong to straight lines issuing from the fixed point. While for $\delta_\sigma = 0$ every point of the region R_σ is fixed, and the fixed points are so-called stable but not attracting.

Then we can see the conditions leading a point P^*_σ to belong to the related region R_σ. For the vertex P^*_L we have:

$$
\begin{cases}
T_1(P^*_L) = a_L - a_M + c_L - c_M > 0,\\
T_2(P^*_L) = a_L - a_R + c_L - c_R > 0,
\end{cases}
\tag{10}
$$

for the vertex P^*_M we have:

$$
\begin{cases}
T_1(P^*_M) = c_L - c_M < 0,\\
T_3(P^*_M) = c_R - c_M < 0,
\end{cases}
\tag{11}
$$

for the vertex P^*_R we have:

$$
\begin{cases}
T_2(P^*_R) = b_L - b_R + c_L - c_R < 0,\\
T_3(P^*_R) = b_R - b_M + c_R - c_M > 0,
\end{cases}
\tag{12}
$$

which ends the proof. □

This proposition allows us to generalize some of the results discussed in [10, p. 403]. In fact, with Proposition 2 we have sufficient conditions for respectively all-Right, all-Middle and all-Left equilibria. This is the analogous of Schelling's case in binary choices of coexistence of all-Right and all-Left equilibria. In the following example we illustrate a case in ternary choices which leads to coexistence of three stable equilibria.

Example 1. Consider the following payoff functions:

$$
L(\mathbf{x}) = x^L, \quad M(\mathbf{x}) = -x^L - x^R + 1, \quad R(\mathbf{x}) = x^R, \tag{13}
$$

then we have:

$$
\begin{aligned}
&T_1(\mathbf{x}) = L(\mathbf{x}) - M(\mathbf{x}) = 2x^L + x^R - 1,\\
&T_2(\mathbf{x}) = L(\mathbf{x}) - R(\mathbf{x}) = x^L - x^R,\\
&T_3(\mathbf{x}) = R(\mathbf{x}) - M(\mathbf{x}) = x^L + 2x^R - 1.
\end{aligned}
$$

In this case the map to be studied is (9) with the following regions:

$$
\begin{aligned}
R_L &= \left\{\mathbf{x} \in D^2 : \quad 1 - 2x^L < x^R < x^L\right\},\\
R_M &= \left\{\mathbf{x} \in D^2 : \quad x^R < \min\left(1 - 2x^L, \frac{1}{2} - \frac{x^L}{2}\right)\right\},\\
R_R &= \left\{\mathbf{x} \in D^2 : \quad x^R > \max\left(x^L, \frac{1}{2} - \frac{x^L}{2}\right)\right\}.
\end{aligned}
\tag{14}
$$

The conditions given in Proposition 2 hold, therefore we have three stable equilibria whose basins of attraction are illustrated in Fig. 2. In Fig. 2(a) we show (at $\delta_L = 0.3$, $\delta_M = 0.2$, and $\delta_R = 0.7$) the three different regions which also correspond to the basins of attraction with three stable equilibria. In Fig. 2(b) three trajectories are shown, which are converging to the three stable equilibria at the vertices.

As mentioned above, Example 1 generalizes to three equilibria the case of coexistence of all-Right and all-Left equilibria in [10]. In our example we have the coexistence of the three unanimity equilibria which are equivalent in terms of payoff. Yet it is not difficult to have other situations with the coexistence of three equilibria which are not equivalent in terms of payoffs. For example, considering the payoff functions $L(\mathbf{x}) = x^L$, $M(\mathbf{x}) = -x^L - x^R + 1$ and $R(\mathbf{x}) = 2x^R$, we still have the coexistence of three unanimity equilibria, where the all-Right one provides a higher payoff and therefore is preferred. Still if either everybody chooses Left or everybody chooses Middle, nobody is motivated to choose otherwise, unless enough others do so to have the population entering the region where Right dominates.

As a consequence of Proposition 2 we have that, depending on the shape and number of regions covering D^2, we can have all the possibilities: either all three equilibria belong to D^2, or only two, or only one, or no fixed points belong to D^2.

In the examples of this section we have seen cases in which all three equilibria coexist. Clearly also the case of only two regions in D^2 and coexistence of two stable fixed points can occur. However, this case is less interesting, as the same as those of a binary choice.

A more relevant case is the coexistence of a stable fixed point with a stable cycle, that we shall see in the next section.

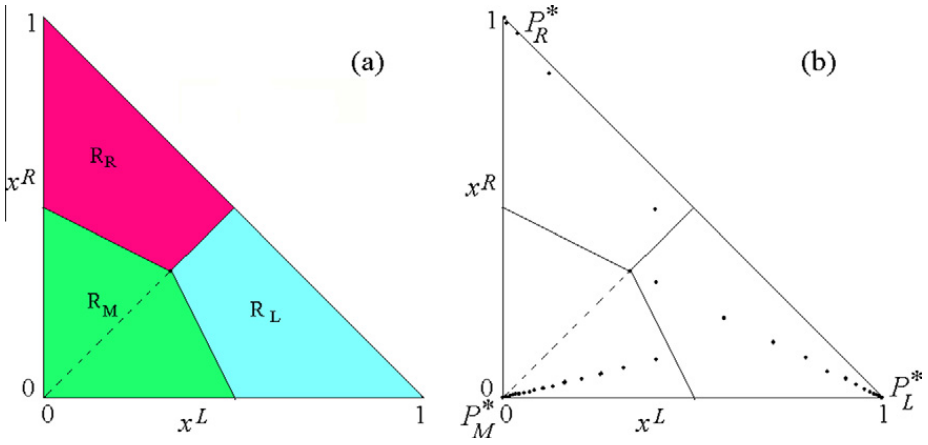

Fig. 2. In (a) the three regions of Example 1, which are also basins of attraction of the three stable equilibria, at $\delta_L = 0.3$, $\delta_M = 0.2$, and $\delta_R = 0.7$. In (b) three different converging trajectories.

4. Coexistence of stable equilibria and k – cycles, $k > 1$

In this section we shall illustrate a few examples in which we always have bistability. This occurs whenever we have one fixed point belonging to its proper region, while something else occurs when the vector $\mathbf{x}_t = (x_t^L, x_t^R)$ belongs to one of the other two regions, thus leading to bistability. In general, we can have coexistence with any single stable equilibria, when:

$$P_\sigma^* \in R_\sigma \quad \text{holds for only one } \sigma \in \{L, M, R\},$$

and the other two regions have a non empty intersection with D^2 and are without fixed point (that is, the relative equilibrium points must be outside each of these two regions). This implies (due to the structure of the map) that periodic orbits (i.e. k-cycles of any period k) exist in the other two regions without fixed points. To clarify this situation let us consider the following example.

Example 2. Consider the payoff functions defined as:

$$L(\mathbf{x}) = x^L, \quad M(\mathbf{x}) = x^R, \quad R(\mathbf{x}) = -x^L - x^R + \alpha \tag{15}$$

with $\alpha \geqslant 1$. Then we have:

$$T_1(\mathbf{x}) = L(\mathbf{x}) - M(\mathbf{x}) = x^L - x^R,$$
$$T_2(\mathbf{x}) = L(\mathbf{x}) - R(\mathbf{x}) = 2x^L + x^R - \alpha,$$
$$T_3(\mathbf{x}) = R(\mathbf{x}) - M(\mathbf{x}) = -x^L - 2x^R + \alpha.$$

In this case the map to be studied is (9) and for $\alpha = 1.5$ we have the following regions:

$$R_L = \left\{\mathbf{x} \in D^2 : x^L \in \left[\frac{1}{2}, 1\right], \ \frac{3}{2} - 2x^L < x^R < x^L\right\},$$
$$R_M = \left\{\mathbf{x} \in D^2 : \ x^L \in \left[0, \frac{1}{2}\right], \ x^R > \frac{3}{4} - \frac{x^L}{2}\right\},$$
$$R_R = \left\{\mathbf{x} \in D^2 : \ x^L \in \left[0, \frac{3}{4}\right], \ x^R < \min\left(\frac{3}{2} - 2x^L, \frac{3}{4} - \frac{x^L}{2}\right)\right\}. \tag{16}$$

The regions R_L, R_M, and R_R are represented in Fig. 3(a) at $\delta_L = 0.75$, $\delta_M = 0.5$, and $\delta_R = 0.3$. One can immediately see that the fixed point P_L^* belongs to its region, and thus it is an attracting fixed point, while the other fixed points P_R^* and P_M^* are not in the proper regions, thus they are virtual (i.e. in this case they are not fixed points of the map). Thus, what is the dynamics of the vector $\mathbf{x}_t = (x_t^L, x_t^R)$ when it belongs to the other two regions? From the definition of the map we can see that if we consider an initial condition in the region R_M the state variable x_t^L will decrease, as $x_{t+1}^L = (1 - \delta_M)x_t^L$. Similarly if we consider an initial condition in the region R_R the state variable x_t^L will decrease, as $x_{t+1}^L = (1 - \delta_R)x_t^L$. It follows that the asymptotic behavior necessarily leads to $x^L = 0$. This means that the dynamics will necessarily converge to some attracting set belonging to the vertical line of the state space, where only x^R varies, and it necessarily follows the asymptotic behavior of the one-dimensional map defined by the dynamics of this variable in the related regions, that is:

$$f: \quad x_{t+1}^L = \begin{cases} f_M(x_t^R) = (1 - \delta_M)x_t^R & \text{if} \quad \frac{3}{4} < x_t^R < 1, \\ f_R(x_t^R) = (1 - \delta_R)x_t^R + \delta_R & \text{if} \quad 0 \leqslant x_t^R < \frac{3}{4}. \end{cases} \tag{17}$$

At the parameter values of Fig. 3(a) the trajectories converge to a 4-cycle, and the shape of the one-dimensional map f is as shown in Fig. 3(b).

This means that independently on the values of the parameters δ_L, δ_M and δ_R, the qualitative behavior can be described as follows: the stable fixed point P_L^* (whose basin of attraction is the related region R_L) coexists with an attracting k-cycle belonging to the line of equation $x^L = 0$ (whose basin of attraction is the region $R_R \cup R_M$). The period k can be any positive integer, and several different cycles also exist with the same period but different periodic points, i.e. having a different number of periodic points on the right and left side of the discontinuity between the two branches f_M and f_R.

In this case, at any fixed value of δ_L we have a one-dimensional piecewise linear map with one discontinuity point, depending on two parameters δ_M and δ_R which give the slopes of the two linear pieces. This map has been already investigate in [3]. Due to the fact that the slopes are less than 1 in modulus, we have that no unstable cycle can exist (and thus no chaos at all). The asymptotic dynamics can only converge to a cycle (periodic orbit of any period

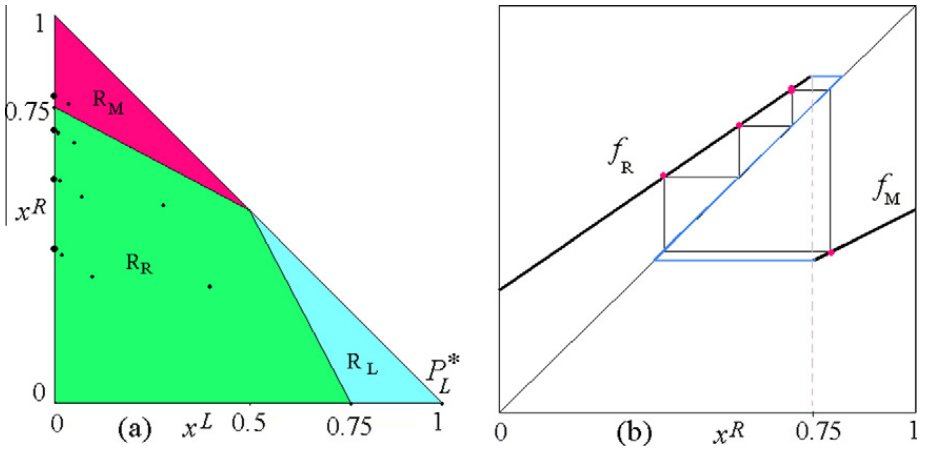

Fig. 3. In (a) regions associated with Example 2 in (15) at $\alpha = 1.5$, $\delta_L = 0.75$, $\delta_M = 0.5$, and $\delta_R = 0.3$. The attracting set is a cycle of period 4. In (b) the map f given in (17) at the same parameters as in (a), showing the attracting 4-cycle.

$k > 1$), or be quasiperiodic in the absorbing interval bounded by the two offsets at the discontinuity point: $I = [f_M(d), f_R(d)]$ where $d = 0.75$ in the example of Fig. 3.

The change in the period of the attracting cycle can only occur via border collision bifurcations (BCB), and the bifurcation curves can be detected analytically. It is proved that two different cycles cannot coexist, and the periodicity regions follow the so-called *period adding structure*. This means that between two periodicity regions of cycles of period p and q also the regions of an attracting cycle of period $(p + q)$ exists, and it is also possible to obtain the analytical expression of the border collision bifurcation curves that bound the periodicity tongues in the parameters plane, of any level of complexity (as is called the organization used to get all the infinitely many cycles). For more details we refer to [6,1].

An example for our map is shown in Fig. 4(a). Notice that it represents both the bifurcation diagram of the one-dimensional map f in (17) and the bifurcation diagram of the two-dimensional map of Example 2 in (15). The cycle of f coexists with the stable fixed point for $\overline{F}$. An example of the periodic orbits existing in the vertical line $x^L = 0$ as a function of only one parameter δ_R is shown in the bifurcation diagram of Fig. 4(b), keeping fixed the other parameters at $\delta_L = 0.75$, $\delta_M = 0.5$, and following the vertical path shown in Fig. 4(a). We can see that the attracting set is a periodic orbit (structurally stable, which means that it is attracting for parameter values always in an interval) and the periods change quickly as a function of the parameter tending to zero (so that one slope tends to 1).

Another example, with a different constant in the function in (15), is shown considering the value $\alpha = 1$. Then we have the following regions:

$$\begin{aligned} R_L &= \{\mathbf{x} \in D^2 : \quad 1 - 2x^L < x^R < x^L\}, \\ R_M &= \left\{\mathbf{x} \in D^2 : \quad x^R > \max\left(x^L, \frac{1}{2} - \frac{x^L}{2}\right)\right\}, \\ R_R &= \left\{\mathbf{x} \in D^2 : \quad x^R < \min\left(1 - 2x^L, \frac{1}{2} - \frac{x^L}{2}\right)\right\}. \end{aligned} \tag{18}$$

The regions R_L, R_M, and R_R are represented in Fig. 5(a) at $\delta_L = 0.75$, $\delta_M = 0.5$, and $\delta_R = 0.3$. Clearly also here the fixed point P_L^* belongs to its region.

In this case the asymptotic dynamics on the vertical line where only x^R varies, follow the asymptotic behavior of the one-dimensional map defined by the dynamics of this variable in the related regions, that is:

$$f: \quad x_{t+1}^R = \begin{cases} f_M(x_t^R) = (1 - \delta_M)x_t^R & \text{if} \quad \frac{1}{2} < x_t^R < 1, \\ f_R(x_t^R) = (1 - \delta_R)x_t^R + \delta_R & \text{if} \quad 0 \leqslant x_t^R < \frac{1}{2}. \end{cases} \tag{19}$$

With respect to the previous case, the asymptotic dynamics are determined by the same map with a different position of the discontinuity point. But except for a change of variable the two cases have the same results, that is the two maps given in (17) and in (19) are topologically conjugated. Also the border collision bifurcations curves are related via an homeomorphism. For example, at $\delta_L = 0.75$ fixed, a two-dimensional bifurcation diagram as a function of δ_M and δ_R is shown in Fig. 5(b). The attractor at $\delta_M = 0.5$ and $\delta_R = 0.3$ is a 5-cycle, as shown in Fig. 5(a).

The cycles observed in this family of examples are similar to the oscillatory behavior observed in [2], and, as already remarked, the two-dimensional bifurcation diagrams (and related dynamics) of this family are identical to those considered in [3]. The difference is that, while in the previous papers the model was for binary choices, here we are considering ternary choices, and the observed cycles are coexisting with an attracting fixed point P_L^*. Thus Example 2 shows that when considering more than two choices there may be coexistence of the stable equilibria and the cyclic behavior studied in the discrete time mathematical formalization by Schelling [10]. It is possible to link this example to the illustration provided in [9]. In fact, assume that agents may use either ponies or bicycle as a means of transportation. We add the further alternative to choose between two different colors of bicycles. Those whose previous choose was ponies keep having the same preference, but those who preferred bicycles may now want to distinguish themselves choosing at each period the less common color. Then, if the number of agents riding ponies is large enough, everybody will ride ponies as all roads will become not viable by bicycles. On the other hand, if the number of agents riding bicycle is large enough everybody will do so, with the color switching dynamics.

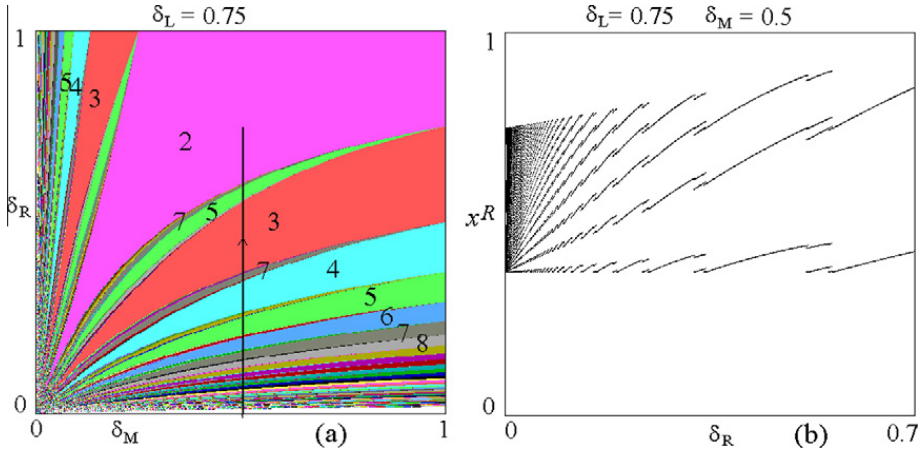

Fig. 4. In (a) two-dimensional bifurcation diagram in the (δ_M, δ_R) plane for Example 2 in (15) and for the map f given in (17) at $\alpha = 1.5$, $\delta_L = 0.75$. Different colors correspond to periodicity regions of cycles with different periods. In (b) the one-dimensional bifurcation diagram of x^R as a function of δ_R along the vertical path shown in (a), at $\delta_M = 0.5$.

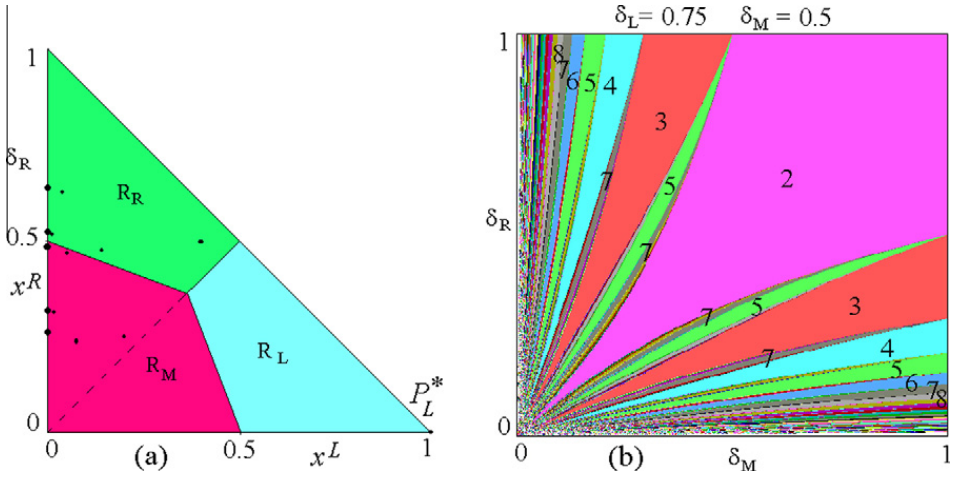

Fig. 5. In (a) regions associated with Example 2 in (15) at $\alpha = 1$, $\delta_L = 0.75$, $\delta_M = 0.5$, and $\delta_R = 0.3$. The attracting set is a cycle of period 5. In (b) two-dimensional bifurcation diagram in the (δ_M, δ_R) plane for Example 2 in (15) and for the map f given in (19) at $\alpha = 1$, $\delta_L = 0.75$.

4.1. Coexistence with non connected basins

A different example of coexistence, in which the basins are disconnected, is given as follows:

Example 3. Assume that the payoff functions are:

$$L(\mathbf{x}) = -x^L + x^R, \quad M(\mathbf{x}) = \alpha, \quad R(\mathbf{x}) = x^L - x^R \tag{20}$$

with $\alpha \in (0,1)$. Then we have:

$$T_1(\mathbf{x}) = L(\mathbf{x}) - M(\mathbf{x}) = -x^L + x^R - \alpha,$$
$$T_2(\mathbf{x}) = L(\mathbf{x}) - R(\mathbf{x}) = -2x^L + 2x^R,$$
$$T_3(\mathbf{x}) = R(\mathbf{x}) - M(\mathbf{x}) = x^L - x^R - \alpha,$$

and the map to be studied is (9) with the following regions:

$$R_L = \left\{\mathbf{x} \in D^2 : \quad x^R > x^L + \alpha\right\};$$
$$R_M = \left\{\mathbf{x} \in D^2 : \quad x^L - \alpha < x^R < x^L + \alpha\right\}; \tag{21}$$
$$R_R = \left\{\mathbf{x} \in D^2 : \quad x^R < x^L - \alpha\right\}.$$

The extension of the regions depends on the value of α. In particular, region R_M is a strip (centered on the line $x^L = x^R$) whose width depends on α. The other regions R_L and R_R are on opposite sides of the strip R_M and the fixed points do not belong to the related regions. The case shown in Fig. 6(a) is with $\alpha = 0.03$.

It is clear that, given the structure of the map, if we take an initial condition in the region R_M the trajectory will converge to the stable fixed point P_M^*, and thus its basin of attraction includes for sure this region. But as before we are interested also in the dynamics occurring for points in the other two regions. An example is shown in Fig. 6(b), at $\delta_L = 0.6$, $\delta_M = 0.5$, and $\delta_R = 0.25$: any initial condition in the white region of D^2 leads to an attracting 3-cycle belonging to the diagonal (of equation $x^R = -x^L + 1$). However not all the points of $R_R \cup R_L$ are converging to this 3-cycle. In Fig. 6(b) we show in green other strips of points whose trajectory is convergent to the stable fixed point P_M^*.

This is an important property of the map which can be explained. In fact, from the structure of our map in (9) we

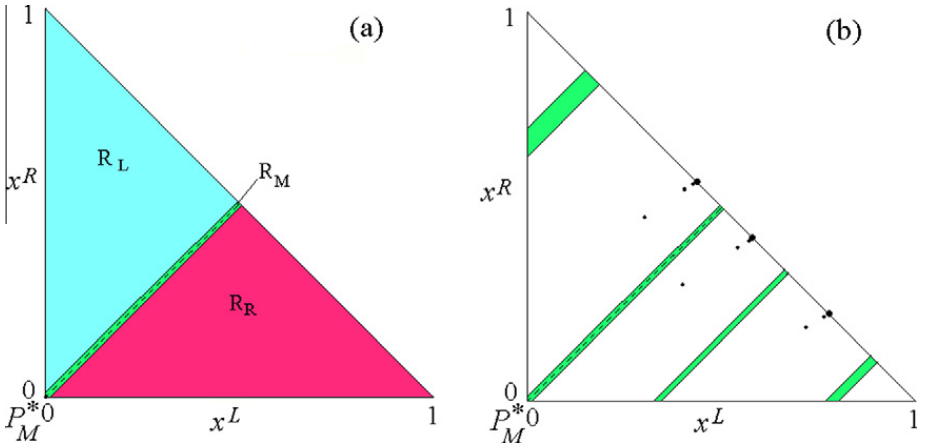

Fig. 6. In (a) regions associated with Example 3 at $\alpha = 0.03$, $\delta_L = 0.6$, $\delta_M = 0.5$, and $\delta_R = 0.25$. The attracting set is a cycle of period 3 shown in (b), where it is also shown, in color, the basin of attraction of the stable fixed point P_M^*.

see that we can consider the dynamics of the state variable:

$$z = x^R - x^L \tag{22}$$

which becomes governed by the one-dimensional map Z given by

$$Z: \quad z_{t+1} = \begin{cases} f_L(z_t) = (1-\delta_L)z_t - \delta_L & \text{if} \quad \alpha < z_t \leqslant 1, \\ f_M(z_t) = (1-\delta_M)z_t & \text{if} \quad -\alpha < z_t < \alpha, \\ f_R(z_t) = (1-\delta_R)z_t + \delta_R & \text{if} \quad -1 \leqslant z_t < -\alpha. \end{cases} \tag{23}$$

The dynamics of this one-dimensional map may represent the asymptotic behaviors of the two-dimensional map of Example 3 in (20). The asymptotic state of (23) in the regions where the functions f_L and f_R are defined is, when existing, an attracting $k-$cycle which coexists with the stable fixed point in $z = 0$. This $k-$cycle corresponds to an attracting cycle of the two-dimensional map, existing on the diagonal, and coexisting with the stable fixed point P_M^*. The one-dimensional map (23) also gives the basin of attraction of the fixed point and (by complement) the basin of the other cycle. The parameters used in the example shown in Fig. 6(b), at $\delta_L = 0.6$, $\delta_M = 0.5$, and $\delta_R = 0.25$, are used in Fig. 7 to illustrate the stable 3-cycle, coexisting with the stable fixed point in $z = 0$ (corresponding to P_M^*). The basin of the fixed point in the origin is obtained by taking all the existing preimages of the segment $(-\alpha, \alpha)$, which in this case are three more segments (in green in Fig. 7), and represent the intersection with the diagonal $x^R = -x^L + 1$ of the basin of P_M^* in D^2.

In this case the dynamics of the map Z (23), and thus the dynamics of Example 3 in (20), lead to a different kind of bistability, with respect to those of Example 2. A difference is clearly due to the structure of the basin, which here is necessarily disconnected. However, the main difference is due to the structure of the one-dimensional map representing the bifurcations: with two discontinuity points here, with only one discontinuity in Example 2. While in Example 2 all the cycles necessarily exist in some periodicity region (and the regions follows the period adding scheme), in the present case, the middle branch of the

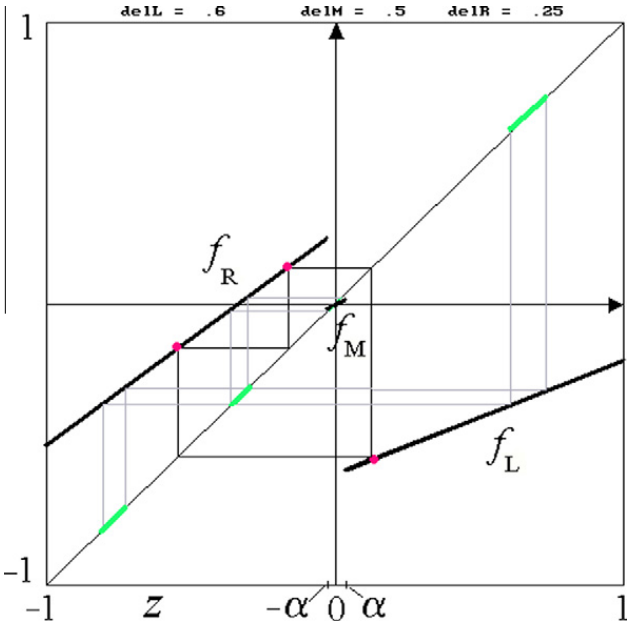

Fig. 7. One-dimensional map (23) at the parameters used in Fig. 6. The attracting sets are a 3-cycle and the origin. In green the basin of attraction of the origin. (For interpretation of the references to colour in this figure legend, the reader is referred to the web version of this article.)

map Z (23) implies that several $k-$cycles now cannot exist. The appearance/disappearance of the existing cycle is always due to a border collision with one of the discontinuity points ($z = -\alpha$ and $z = \alpha$), but all the preimages of this middle branch lead to the destruction of many $k-$cycles. Two examples of the bifurcation diagrams occurring in this family are shown in Fig. 8. They have been numerically computed for the two-dimensional Example 3 in (20) at two different values of α and it is clearly identical to the bifurcation diagram numerically computed for the map Z in (23). As we can see, increasing the parameter α the basin of attraction of the fixed point in the origin also increases, leading to the disappearance via border collision bifurcation of more and more cycles. The two-dimensional bifurcation diagram in Fig. 8(b) shows the disappearance of many periodicity regions, and the destruction of the adding

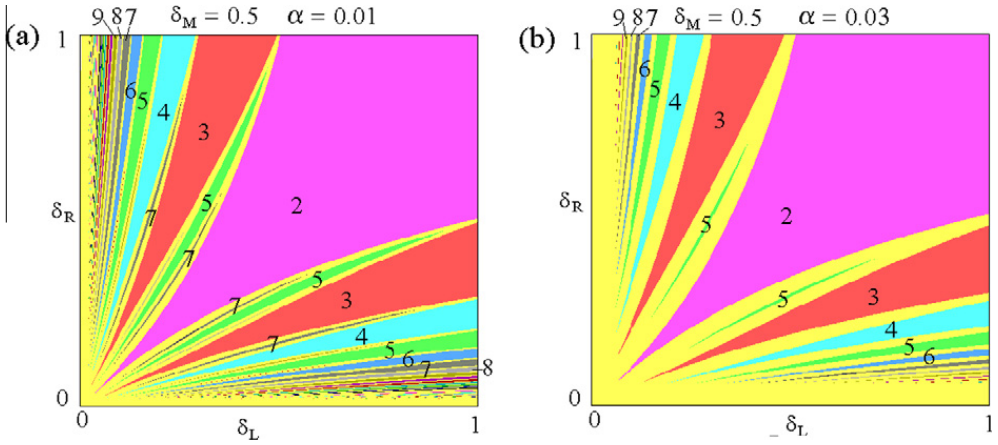

Fig. 8. Two-dimensional bifurcation diagram in the (δ_L, δ_R)-plane for the map of Example 3 in (20) and for the map f given in (23) at $\alpha = 0.01$ in (a), $\alpha = 0.03$ in (b), and $\delta_L = 0.75$. The initial condition is $(x^L, x^R) = (0.45, 0.55)$. The yellow points represent convergence to the origin. (For interpretation of the references to colour in this figure legend, the reader is referred to the web version of this article.)

structure. When α is big enough all the other cycles disappear, leading to a unique stable fixed point in the origin.

So, even if Example 3 is apparently quite similar to Example 2 in terms of coexistence of stable fixed point and cycles, there are some important differences. In fact, in the latter we can observe the transition from the cyclic behavior which characterizes binary choices with overshooting [2] to the stable fixed point in [10]. Example 3 shows that there are situations in which the two behaviors observed for binary choices coexist but not as in Example 2 where we could decompose a *3*-choice problem as a *2*-choice plus one more. In the next section we show how considering ternary choices the behavior can be radically different from what has been observed for binary choices.

5. The case of no stable equilibria

In this section we shall see how new kinds of dynamics can occur in the ternary choices, when the parameters of the model are such that no stable equilibria exist. In order to investigate this case, in which no fixed point belongs to the related dominance region, i.e. $P^*_\alpha \notin R_\alpha$ for any α, we consider the following example.

Example 4. Let the payoff functions be given by

$$L(\mathbf{x}) = x^R, \quad M(\mathbf{x}) = -\frac{1}{2}x^R + \frac{4}{5}, \quad R(\mathbf{x}) = -x^R + 1, \tag{24}$$

then we have:

$$\begin{aligned} T_1(\mathbf{x}) &= L(\mathbf{x}) - M(\mathbf{x}) = \frac{3}{2}x^R - \frac{4}{5}, \\ T_2(\mathbf{x}) &= L(\mathbf{x}) - R(\mathbf{x}) = 2x^R - 1, \\ T_3(\mathbf{x}) &= R(\mathbf{x}) - M(\mathbf{x}) = -\frac{1}{2}x^R + \frac{1}{5}, \end{aligned} \tag{25}$$

and the map to be studied is (9) with the following regions:

$$\begin{aligned} R_L &= \left\{\mathbf{x} \in D^2 : \ \frac{8}{15} < x^R \leqslant 1\right\}, \\ R_M &= \left\{\mathbf{x} \in D^2 : \ \frac{2}{5} < x^R < \frac{8}{15}\right\}, \\ R_R &= \left\{\mathbf{x} \in D^2 : \ 0 \leqslant x^R < \frac{2}{5}\right\}. \end{aligned} \tag{26}$$

From the definition of the regions, it is immediately evident that now the state variable x^R is decoupled from x^L. So all the bifurcations of the system can be investigated via the one-dimensional map $x^R_{t+1} = f(x^R_t)$ given by

$$f: \quad x^R_{t+1} = \begin{cases} f_L(x^R_t) = (1-\delta_L)x^R_t & \text{if} \quad \frac{8}{15} < x^R_t \leqslant 1, \\ f_M(x^R_t) = (1-\delta_M)x^R_t & \text{if} \quad \frac{2}{5} < x^R_t < \frac{8}{15}, \\ f_R(x^R_t) = (1-\delta_R)x^R_t + \delta_R & \text{if} \quad \leqslant x^R_t < \frac{2}{5}, \end{cases} \tag{27}$$

and the values of the other variable depend on the following function h:

$$h: \quad x^L_{t+1} = \begin{cases} h_L(x^L_t) = (1-\delta_L)x^L_t + \delta_L & \text{if} \quad \frac{8}{15} < x^R_t \leqslant 1, \\ h_M(x^L_t) = (1-\delta_M)x^L_t & \text{if} \quad \frac{2}{5} < x^R_t < \frac{8}{15}, \\ h_R(x^L_t) = (1-\delta_R)x^L_t & \text{if} \quad 0 \leqslant x^R_t < \frac{2}{5}. \end{cases} \tag{28}$$

The dynamic behavior of the state variable x^R depends on a discontinuous map with three branches, each one representing a region of D^2, and the existing cycles may have periodic points on three partitions. This example differs from the one-dimensional map that we have seen in the previous section, also with three partitions. In fact, while for the map in (23) the branch in the middle has a stable fixed point, *in the one here considered there are no fixed points*. This makes a great difference in the dynamic behavior.

As we already know, the peculiarity of the one-dimensional map f in (27) is that the conditions on the parameters determining the slopes of the linear pieces lead to all contractions for the single functions f_i. Under such conditions we can only have stable cycles as persistent attractors (i.e. structurally stable) or quasiperiodic trajectories (at structurally unstable parameter constellations), because all the slopes are positive and less than one, so that any possible k – periodic cycle has an eigenvalue which is necessarily positive and smaller than one[3]. Thus, as already remarked, no chaotic behavior can occur. This kind of

[3] We recall that the eigenvalue of a cycle is the product of the slopes of the function in the periodic points.

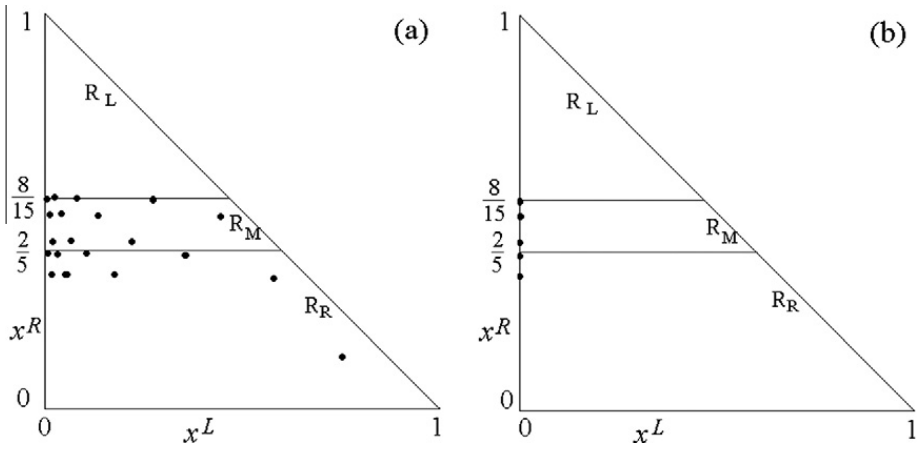

Fig. 9. Stable cycles in the phase plane (x^L, x^R). In (a) a period 20 stable cycle. In (b) a period 5 stable cycle.

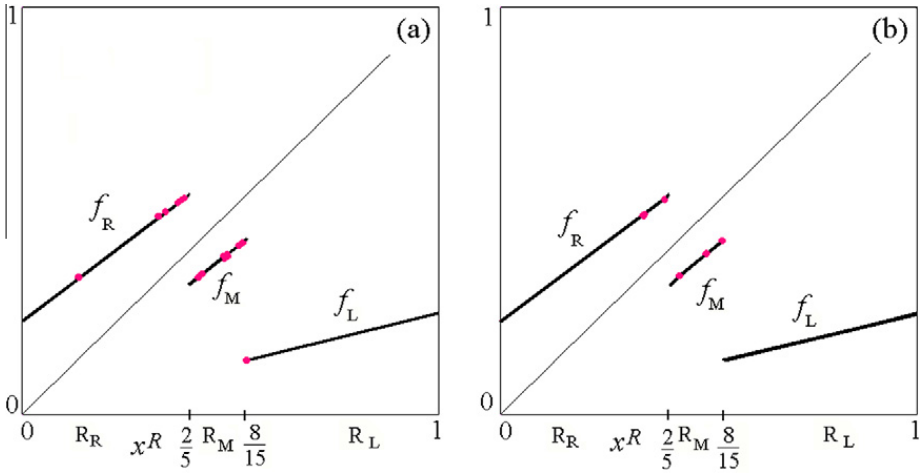

Fig. 10. One-dimensional map f. In (a) and (b) at the same parameter values as in Fig. 9(a) and (b), respectively.

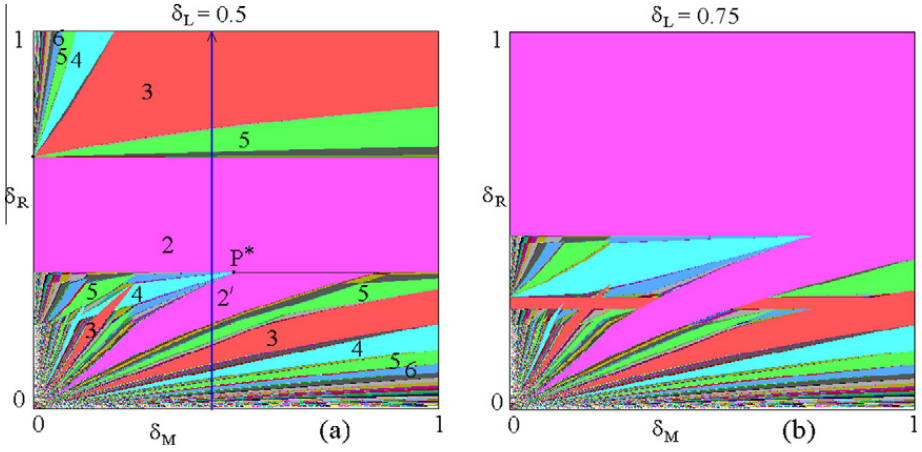

Fig. 11. Two-dimensional bifurcation diagram in the (δ_L, δ_R)-plane for Example 4 in (24) and for the map f given in (27) at $\delta_L = 0.5$ in (a) and $\delta_L = 0.75$ in (b).

one-dimensional maps, with two discontinuity points, has been recently considered in [11], and in our model we shall find results similar to those described in the cited paper (with periodicity regions following particular adding structures).

The existing cycles may have periodic points either belonging to all the three partitions (leading to truly new ternary choices), or to only two partitions. A few attracting sets of the two-dimensional map (9) in this specific case (24) can be seen in Fig. 9. In Fig. 9(a) we show a stable cycle of period 20 at $\delta_L = 0.75$, $\delta_M = 0.2$, $\delta_R = 0.23$, having periodic points in the three partitions. In Fig. 9(b), after a small variation of δ_R, at $\delta_R = 0.229$, a stable cycle of period 5 exists,

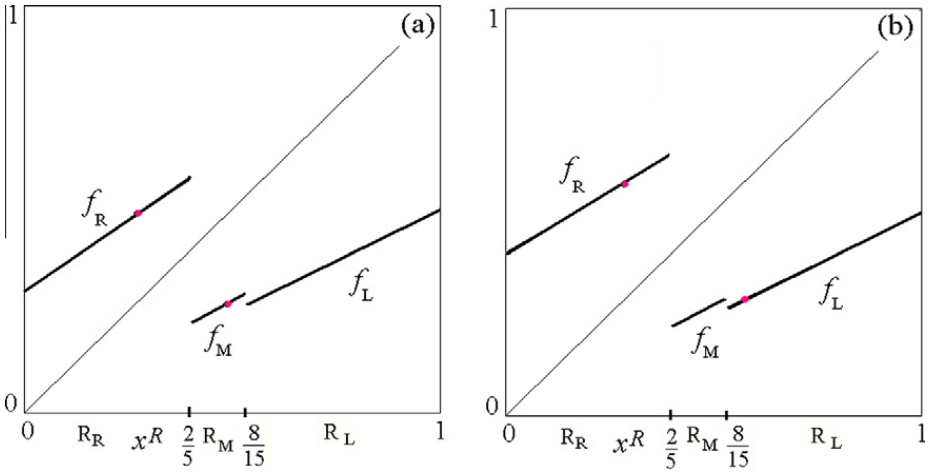

Fig. 12. Two coexisting cycles of period 2 at $\delta_L = 0.5$, $\delta_M = 0.45$, $\delta_R = 0.3$. In (a) two periodic points are $x^R = 0.2683$ and $x^R = 0.4878$. In (b) two periodic points are $x^R = 0.2857$ and $x^R = 0.5714$.

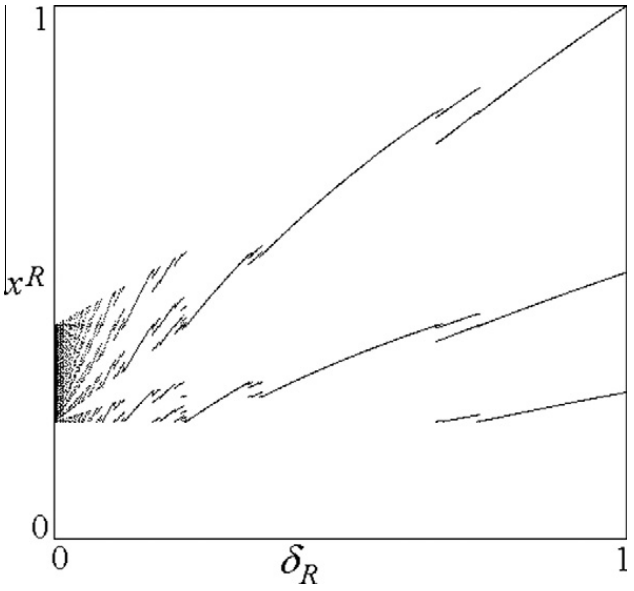

Fig. 13. One-dimensional bifurcation diagram of x^R as a function of δ_R along the vertical path shown in Fig. 11(a).

with periodic points only in two partitions. The bifurcation occurring from Fig. 9(a) to b is a border collision bifurcation due to the merging of a periodic point of the 20-cycle with the border $x^R = \frac{8}{15}$ where the map changes its definition.

The example shown in Fig. 9 shows that, after the bifurcation leading from the attracting set of Fig. 9(a) to that of Fig. 9(b), we have not only an attracting cycle of different period, but also with asymptotic points on the line $x_t^L = 0$. That is, while in the *20*-cycle we have periodic points leading to vectors (x_t^R, x_t^L, x_t^M) with three non zero components and $x_t^M = 1 - x_t^R - x_t^L$, in the *5*-cycle the states are: $(x_t^R, x_t^M, 0)$, with $x_t^M = 1 - x_t^R$ (and we return in a 2-choice case).

As mentioned above, this kind of bifurcation is due to the fact that the *20*-cycle shown in Fig. 9(a) has periodic points in all the three regions, while after a small perturbation of the parameter δ_R (leading to a border collision) the *5*-cycle shown in Fig. 9(b) has periodic points only in two regions: R_M and R_R. The reason why of this dynamic behavior can be immediately understood making use of the one-dimensional map f given in (27). In Fig. 10 we show its graph at the same parameters' values as those of Fig. 9. We see that the maximum value is taken from the offset of the function $f_R(x_t^R)$ in the discontinuity point $x^R = \frac{2}{5}$, as in fact the asymptotic dynamics occur in the absorbing interval given by $I = [f_L(\frac{8}{15}), f_R(\frac{2}{5})]$, which includes all the three regions. However a periodic point is very close to the second discontinuity point, that is, very close to its border collision bifurcation. This bifurcation has already occurred when the parameters are as those in Fig. 9(b), and the map becomes as in Fig. 10(b). The 5-cycle belongs now to an absorbing interval given by $I = [f_M(\frac{2}{5}), f_R(\frac{2}{5})]$, which includes only one discontinuity point and involves only two regions (R_M and R_R).

The kind of bifurcation diagrams which characterize our map can be observed in Fig. 11: when fixing $\delta_L = 0.5$ and $\delta_L = 0.75$ we can draw a two-dimensional bifurcation diagram in the parameter plane (δ_M, δ_R). The two-dimensional bifurcation diagrams shown in Fig. 11 are exactly the same for the one-dimensional map f and for the two-dimensional map since, as remarked above, the state variable x^R is independent from the other, x^L, and all the bifurcations are due to border collision bifurcations involving also f. Thus we can partially reduce the dimensionality of the map to study, at least regarding the bifurcations, which must necessarily occur in the x^R variable.

As already remarked, for the one-dimensional map f in (27) the asymptotic behavior is necessarily a stable cycle, or (more rarely) a quasiperiodic trajectory, and the changes in the periods can only occur via border collision, i.e. a periodic point which is merging, or colliding, with a discontinuity point, or borderof the definition of the map. However, due to the existence of two discontinuity points, *regions of coexistence of two attracting cycles are possible*, which indeed occur in the overlapping of periodicity regions which are also visible in Fig. 11.

In fact, as remarked in [11], another peculiarity of discontinuous maps with increasing branches and two discontinuities is the possibility of at most two coexisting cycles (this is due to the fact that each cycle must be

associated with a discontinuity point). In the same paper it was also evidenced the existence of particular points, called *big-bang bifurcation points*, which are associated with the intersection of two bifurcation curves. Such points are peculiar because infinitely many border collision bifurcation curves are issuing from them. And in the case of increasing branches (as we have) each big-bang bifurcation point is the issuing point of bifurcation curves which follow the *period adding scheme*. This means that for parameters in any neighborhood of a big-bang bifurcation point we can have a stable cycle of any period. For example, the point P^* in Fig. 11(a) occurs at the intersection of two BCB curves, one associated with a *2*-cycle having periodic points in the branches f_M and f_R (see Fig. 12(a)) and the other associated with a *2*-cycle having periodic points in the branches f_L and f_R, as shown in Fig. 12(b). *This is one more relevant difference with respect to the case of binary choices*.

To appreciate the different periods that the attracting cycles can have, in Fig. 13 a bifurcation diagram of the variable x^R as a function of δ_R is shown, at fixed $\delta_M = 0.45$ and $\delta_L = 0.5$ along the vertical path shown in Fig. 11(a).

This last example shows how considering ternary choices may lead to behaviors that are radically different from those observed for binary choices. In fact, here we can have cyclic behaviors in which all the three states are changing, and also coexistence of two such cycles may occur. The bifurcation diagrams in this case (a map with two discontinuity points) is very much different from those occurring when only one discontinuity exists -a few examples of which have been shown in Section 4.

This means that, when considering the dynamics, the simplifying choice of two alternatives may be too reductive. It is not only the elimination of one alternative *per se* rather, and more important, it careless ignores the underlying complexity.

6. Conclusion

In this paper we have investigated the dynamics of repeated games with three choices, described by two-dimensional models in discrete time, evidencing the differences with respect to models with binary choices. Our analysis has raised interesting findings at least from two different perspectives. The first one involves the applied aspect of the problems and the second one is in terms of bifurcation structures which can be observed.

We have found dynamics that, in some cases, are the analog of those described in the literature about binary choices. In fact, we have shown both situations with the coexistence of unanimity equilibria as described in [10] and also situations with cyclic behaviors as those analyzed in [3]. Furthermore, by introducing a third alternative we can have the coexistence of these two situations. Then we have investigated the case of pure three choices which can be considered as the juxtaposition of two choices to additional one. Further analysis has shown dynamics which are different from those observed for binary choices. The complexity of our Examples 3 and 4 leads to the expected result that ternary choices cannot be simply considered as a binary choice plus one.

As it concerns the dynamics, the analysis of the illustrated examples has evidenced bifurcation structures which were impossible to observe in binary choices. While on one hand we could find also for the ternary choice model the same border collision bifurcation structure (adding scheme) which was analyzed in [3], on the other hand in the last example we have found more complicated bifurcation diagrams, with the existence of big-bang bifurcation points leading to new border collision bifurcation structures. This is something that cannot be found in binary choice models. In particular, we have also described regions in the parameter space associated with overlapping periodicity regions, leading to bistability between two cycles of different periods, none of which is a fixed point.

In future research we will further the analysis along two main avenues. On one hand, it is interesting to analyze the mathematical properties of piecewise linear maps; on the other hand, it would be quite interesting to relax the assumption of impulsive agents introducing other kinds of behavior.

Acknowledgments

This work has been performed within the activity of the PRIN project "Local interactions and global dynamics in economics and finance: models and tools", MIUR, Italy.

References

[1] Avrutin V, Schanz M, Gardini L. Calculation of bifurcation curves by map replacement. Int J Bifurcat Chaos 2010;20(10):3105–35.
[2] Bischi GI, Merlone U. Global dynamics in binary choice models with social influence. J Math Sociol 2009;33:1–26.
[3] Bischi GI, Gardini L, Merlone U. Impulsivity in binary choices and the emergence of periodicity. Discret Dyn Nat Soc 2009. doi:10.1155/2009/407913. ID 407913.
[4] Bischi GI, Gardini L, Merlone U. Periodic cycles and bifurcation curves for one-dimensional maps with two discontinuities. J Dyn Syst Geom Theor 2009;7(2):101–23.
[5] Dixit AK, Skeath S. Games of strategy. 2nd ed. New York: W.W. Norton and Company; 2004.
[6] Gardini L, Tramontana F, Avrutin V, Schanz M. Border collision bifurcations in 1D PWL map and Leonov's approach. Int J Bifurcat Chaos 2010;20(10):3085–104.
[7] Kandori M. Social norms and community enforcement. Rev Econ Stud 1992;59(1):63–80.
[8] Mas-Colell A, Whinston MD, Green JR. Microeconomic theory. New York: Oxford University Press; 1995.
[9] McFadden DL. Quantal choice analysis: a survey. Ann Econ Soc Meas 1976;5(4):363–90.
[10] Schelling TC. Hockey helmets, concealed weapons and daylight saving. J Conflict Resolut 1973;17:381–428.
[11] Tramontana F, Gardini L, Avrutin V, Schanz M. Periodic adding in piecewise linear maps with two discontinuities; International Journal of Bifurcation and Chaos accepted for publication.
[12] Van Vugt M, Van Lange PAM, Meertens RM. Commuting by car or public transportation? A social dilemma analysis of travel mode judgements. Eur J Soc Psychol 1996;26:373–95.
[13] Varian H. Microeconomic analysis. New York: W.W. Norton and Company; 1992.